The *in vitro* antiviral activity of the anti-hepatitis C virus (HCV) drugs daclatasvir and sofosbuvir against SARS-CoV-2

Running-title: SARS-CoV-2 susceptibility to daclatasvir and sofosbuvir in vitro

Carolina Q. Sacramento[1,7#], Natalia Fintelman-Rodrigues[1,7#], Jairo R. Temerozo[2,3], Suelen da Silva Gomes Dias[1], André C. Ferreira[1,4,7], Mayara Mattos[1,7], Camila R. R. Pão[1], Caroline S. de Freitas[1,7], Vinicius Cardoso Soares[1], Fernando A. Bozza[5,6], Dumith Chequer Bou-Habib[2,3], Patrícia T. Bozza[1], Thiago Moreno L. Souza[1,7,*]

# - These authors contributed equally to this work

1 – Laboratório de Imunofarmacologia, Instituto Oswaldo Cruz (IOC), Fundação Oswaldo Cruz (Fiocruz), Rio de Janeiro, RJ, Brazil.

2 – National Institute for Science and Technology on Neuroimmunomodulation (INCT/NIM), IOC, Fiocruz, Rio de Janeiro, RJ, Brazil.

3 – Laboratório de Pesquisas sobre o Timo, IOC, Fiocruz, Rio de Janeiro, RJ, Brazil.

4 - Universidade Iguaçu, Nova Iguaçu, RJ, Brazil.

5 – Instituto Nacional de Infectologia Evandro Chagas, Fiocruz, Rio de Janeiro, RJ, Brazil

6 – Instituto D'or de Pesquisa e Ensino, Rio de Janeiro, RJ, Brazil

7 - National Institute for Science and Technology on Innovation in Diseases of Neglected Populations (INCT/IDPN), Center for Technological Development in Health (CDTS), Fiocruz, Rio de Janeiro, RJ, Brazil.

***Correspondence footnote:**

Thiago Moreno L. Souza, PhD

****

Fundação Oswaldo Cruz (Fiocruz)
Centro de Desenvolvimento Tecnológico em Saúde (CDTS)
Instituto Oswaldo Cruz (IOC), Pavilhão 108, sala 49
Av. Brasil 4365, Manguinhos, Rio de Janeiro - RJ, Brasil, CEP 21060340
Tel.: +55 21 2562-1311

Email: tmoreno@cdts.fiocruz.br

Abstract

The infection by the Severe acute respiratory syndrome coronavirus 2 (SARS-CoV-2) causes major public health concern and economic burden. Although clinically approved drugs have been repurposed to treat individuals with 2019 Coronavirus disease (COVID-19), the lack of safety studies and limited efficiency as well jeopardize clinical benefits. Daclatasvir and sofosbuvir (SFV) are clinically approved direct-acting antivirals (DAA) against hepatitis C virus (HCV), with satisfactory safety profile. In the HCV replicative cycle, daclatasvir and SFV target the viral enzymes NS5A and NS5B, respectively. NS5A is endowed with pleotropic activities, which overlap with several proteins from SARS-CoV-2. HCV NS5B and SARS-CoV-2 nsp12 are RNA polymerases that share homology in the nucleotide uptake channel. These characteristics of the HCV and SARS-CoV-2 motivated us to further study the activity of daclatasvir and SFV against the new coronavirus. Daclatasvir consistently inhibited the production of infectious SARS-CoV-2 virus particles in Vero cells, in the hepatoma cell line HuH-7 and in type II pneumocytes (Calu-3), with potencies of 0.8, 0.6 and 1.1 µM, respectively. Daclatasvir targeted early events during SARS-CoV-2 replication cycle and prevented the induction of IL-6 and TNF-α, inflammatory mediators associated with the cytokine storm typical of SARS-CoV-2 infection. Sofosbuvir, although inactive in Vero cells, displayed EC_{50} values of 6.2 and 9.5 µM in HuH-7 and Calu-3 cells, respectively. Our data point to additional antiviral candidates, in especial daclatasvir, among drugs overlooked for COVID-19, that could immediately enter clinical trials.

1) Introduction

Several single-stranded positive sense RNA viruses affect the public health, causing hepatitis C, dengue, Zika, yellow fever, chikungunya and severe acute respiratory syndrome (SARS). The unfold of the ongoing pandemic of SARS coronavirus (CoV) 2 highlights that the world is ill-prepared to respond to the spillover of highly pathogenic respiratory viruses (1). Indeed, in the two decades of the 21st century, other life-threatening public health emergencies of international concern related to other coronavirus emerged, such as the SARS-CoV in 2002, and the Middle-East respiratory syndrome (MERS-CoV) in 2014 (2). Since the end of 2019 to date, the infection by SARS-CoV-2 has reached 188 countries, affecting more than 7.5 million persons, with mortality ratio of 5-10 % (3).

Despite the self-quarantining and social distancing to avoid contact between infected/uninfected individuals and to diminish transition rates, it has become evident that long-term control and prevention of 2019 CoV disease (COVID-19) will be dependent on effective antivirals and vaccines. In this sense, the repurposing of clinically approved drugs is recognized by the World Health Organization (WHO) as the fastest way to catalogue candidate treatments (4)(5). WHO's global clinical trial (named Solidarity) selected four therapeutic interventions, such as ~~with~~ lopinavir (LPV)/ritonavir (RTV), in combination or not with interferon-β (IFN-β), chloroquine (CQ) and remdesivir (RDV) to treat COVID-19(5). Safety of repurposing antiviral has been an issue for COVID-19 (6, 7), and controversial efficacy of the components of the Solidarity trial has been described (6–8). Nevertheless, very early treatment with RDV showed promising results in non-human primates and clinical studies (7, 9, 10).

Direct-acting antivirals (DDA) against hepatitis C virus (HCV) are among the safest antiviral agents, since they become routinely used in the last five years(11). Due to their recent incorporation amongst therapeutic agents, drugs like daclatasvir and sofosbuvir (SFV) were not systematically tested against SARS-CoV or MERS-CoV.

Daclatasvir inhibits HCV replication by binding to the N-terminus of non-structural protein (NS5A), affecting both viral RNA replication and virion assembly (12). NS5A is a multifunctional protein in the HCV replicative cycle, involved with recruitment of cellular lipidic bodies, RNA binding and replication, protein-phosphorylation, cell signaling and

antagonism of interferon pathways (12). In large genome viruses, such as SARS-CoV-2, these activities are executed by various viral proteins, especially the non-structural proteins (nsp) 1 to 14(13).

SFV inhibits the HCV protein NS5B, its RNA polymerase(14). This drug has been associated with antiviral activity against the Zika (ZIKV), yellow fever (YFV) and chikungunya (CHIKV) viruses(15–18). With respect to HCV, SFV appears to have a high barrier to the development of resistance. SFV is 2`Me-F uridine monophosphate nucleotide(14). Hydrophobic protections in its phosphate allow SFV to enter the cells, and then this pro-drug must become the active triphosphorylated nucleotide. Although the cellular enzymes cathepsin A (CatA), carboxylesterase 1 (CES1) and histidine triad nucleotide-binding protein 1 (Hint1) involved with removal of monophosphate protections are classically associated with the hepatic expression(19), they are also present in other tissue, such as the respiratory tract(20–22). Moreover, the similarities between the SARS-CoV-2 and HCV RNA polymerase suggest that sofosbuvir could act as an antiviral against COVID-19(23). Using enzymatic assays, sofosbuvir was shown to act as a competitive inhibitor and a chain terminator for SARS-CoV-2 RNA polymerase(24, 25). In human brain organoids, sofosbuvir protected from SARS-CoV-2-induced cell death(26).

Altogether, these data motivated us to use cellular-based assays in combination with titration of infectious viral particles and molecular assay to evaluate if the level of susceptibility of SARS-CoV-2 to daclatasvir and SFV would occur in physiologically relevant concentrations. Daclatasvir consistently inhibited the production of infectious SARS-CoV-2 in different cells, targeting early events during viral replication cycle and preventing the induction of IL-6 and TNF-α, inflammatory mediators associated with the cytokine storm characteristic of the SARS-CoV-2 infection. SFV, which was inactive in Vero cells, inhibited SARS-CoV-2 replication more potently in hepatoma than in respiratory cell lines. Our data point to additional antiviral candidates that should be considered for clinical trials and eventual treatment for COVID-19 and to potential chemical structures for efficiency optimization.

2) Results

2.1) SARS-CoV-2 is susceptible to daclatasvir and SFV in a dose- and cell-dependent manner

SARS-CoV-2 may infect cell lineages from different organs, but permissive production of infectious virus particles varies according to the cell type and culture conditions. Since we wanted to diminish infectious virus titers with studied antiviral drugs, we first compared common cell types used in COVID-19 research with respect to their permissiveness to SARS-CoV-2. Whereas African green monkey kidney cell (Vero E6), human hepatoma (HuH-7) and type II pneumocytes (Calu-3) produce infectious SARS-CoV-2 titers and quantifiable RNA levels (Figure S1), A549 pneumocytes displayed limited ability to generate plaque forming units (PFU) of virus above the limit of detection (Figure S1A). Therefore, our next experiments were performed with Vero E6, HuH-7 and Calu-3 cells.

To functionally test whether daclatasvir or SFV would inhibit SARS-COV-2 replication, cells were infected at experimental conditions to reach the peak of virus replication, e.g. MOI of 0.01 for Vero cells or 0.1 to HuH-7 and Calu-3 cells. Cultures were treated with daclatasvir or SFV after infection. After 24 h (Vero) or 48h (HuH-7 and Calu-3) culture supernatants were harvested and infectious SARS-CoV-2 tittered in Vero cell. Daclatasvir inhibited the production of SARS-CoV-2 infectious virus titers in dose-dependent manner (EC_{50} of 0.8 µM; Table 1), but showed no efficiency when virus was quantified by copies/mL (Figures 1A and 1B, S2A and S2B, Table 1). These data strengthen that measurement of virus-induced PFU represents a more reliable way to search for antiviral drugs than quantification of RNA loads.

SFV did not inhibit SARS-CoV-2 replication in Vero cells (Figure 1A and 1B, S2A and S2B). On the other hand, daclatasvir consistently inhibited SARS-CoV-2 replication in Huh-7 and Calu-3 cells with potencies of 0.6 and 1.1 µM, respectively (Figures 1C and D, S2C and S2D, Table 1). SFV was 35 % more potent to inhibit SARS-CoV-2 replication in Huh-7 then in Calu-3 cells (Figures 1C and D, S2C and S2D, Table 1). For comparisons, daclatasvir was 1.1- to 4-fold more potent and efficient than, CQ, LPV/RTV and ribavirin (RBV), used here as positive controls (Figures 1, S2 and Table 1). SFV performed similarly

to RBV to inhibit SARS-CoV-2 production in HuH-7 and Calu-3 cells (Figures 1, S2 and Table 1). Nevertheless, selective index (SI = CC_{50}/EC_{50}) for SFV was 4.6-times superior then RBV, because of SFV`s lower cytotoxicity (Table 1).

These data demonstrated that SARS-CoV-2 is susceptible to daclatasvir and SFV at different magnitudes.

2.2) Daclatasvir and SFV decrease SARS-CoV-2 RNA synthesis.

Different proteins of the SARS-CoV-2 life cycle could be targeted by daclatasvir, which originally targets the multi-functional HCV protein NS5A. To gain insight on the temporality of events critical for daclatasvir`s activity against SARS-CoV-2, we performed time-of-addition (TOA) assays. Vero cells were infected at MOI of 0.01 and treated with two times the EC_{50} of daclatasvir. Vero cells were used in this assay because they present the peak of virus replication in 24 h, and because, for proper readout, it is wise to avoid multiple rounds of re-infection in this experiment.

We found that treatments could be efficiently postponed up to 4h with daclatasvir, declining thereafter (Figure 2A). The temporal preservation of daclatasvir's anti-SARS-CoV-2 activity overlaps with RBV, which inhibits pan-inhibitor of viral RNA synthesis (Figure 2A).

To confirm daclatasvir's effect on viral RNA synthesis, and considering that SFV is a RNA polymerase inhibitor, we next tested if these treatments could impair cell-associated SARS-CoV-2 genomic and subgenomic RNA synthesis in type II pneumocytes (Calu-3 cells). These cells were infected at MOI of 0.1 and treated with 10 μM of the compounds. After two days, cellular monolayers were lysed and real time RT-PCR performed for ORF1 (genomic) and ORFE (subgenomic) RNA quantification. Daclatasvir was two-times more efficient to inhibit viral RNA synthesis when compared to SFV (Figure 2B). Daclatasvir was also more efficient to impair subgenomic RNA synthesis and genomic RNA levels, reinforcing the perception of targeting the SARS-CoV-2 RNA polymerase complex (Figure 2B).

2.3) **Daclatasvir prevents pro-inflammatory cytokine production in SARS-CoV-2-infected monocytes.**

Severe COVID-19 has been associated with increased levels of leukopenia and uncontrolled pro-inflammatory response (27). Viral infection in the respiratory tract often triggers the migration of blood monocytes to orchestrate the transition from innate to adaptive immune responses(28), where the imbalance of pro-inflammatory mediators, such as IL-6 and TNF-α, may result in cytokine storm. We thus infected human primary monocytes with SARS-CoV-2 and found that daclatasvir, the most potent compound observed here, was significantly more efficient to reduce cell-associated RNA levels than the other studied drugs for COVID-19 (Figure 3A). Accordingly, daclatasvir also reduced the SARS-CoV-2-induced enhancement of TNF-α and IL-6 (Figure 3B and C). Our results strongly suggest that the investigated HCV DDA, due to their anti-SARS-CoV-2 and anti-inflammatory effects here described, may offer ~~play~~ a beneficial aspect role for patients with COVID-19.

3) Discussion

The COVID-19 has become a major global health threaten, and most significant economic burden in decades(29). On June 15th, around 6 months after the outbreak in Wuhan, China, the WHO recorded more than 7.5 million cases and 420,000 deaths worldwide (2). SARS-CoV-2 is the third highly pathogentic coronavirus that emerged in these two decades of the 21st century (2). SARS-CoV-2 actively replicates in type II pneumocytes, leading to cytokine storm and the exacerbation of thrombotic pathways (27, 30, 31). This virus-triggered sepsis-like disease associated with severe COVID-19 could be blocked early during the natural history of infection with antivirals (27, 30, 31). Indeed, clinical studies providing early antiviral intervention accelerated the decline of viral loads and diminished disease progression(9, 10). The decrease of viral loads is an important parameter, because it could reduce the transmissibility at the treated individual level.

To rapidly respond to an unfolded pandemics, it is pivotal to catalogue preclinical data on the susceptibility of SARS-CoV-2 to clinically approved drugs, as an attempt to trigger clinical trials with promising products (4). We used this approach during ZIKV, YFV, and CHIKV outbreak in Brazil, when we showed the susceptibility of these viruses to SFV (15–18, 32). SFV and dacaltasvir are considered safe anti-HCV therapy with potential to be used with broader antiviral activity. Here, we demonstrated that SARS-CoV-2 is susceptible to daclatasvir, across different cell types tested, and to SFV, in a cell-dependent manner. In line with their activity against HCV, these drugs impaired SARS-CoV-2 RNA synthesis.

In the 9.6 kb genome of HCV, the gene *ns5a* encodes for a multifunctional protein. The protein NS5A possesses motifs involved with lipid, zinc and RNA biding, phosphorylation and interaction with cell signaling events(12). In other viruses, with less compact genomes, the functions and motifs present in NS5A are distributed to other proteins. For instance, in SARS-CoV-2, its 29 kb genome encodes for nsp3, with zinc motif; nsp4 and 5, with lipidic binding activity; nsp7, 8, 12, 13 and 14 able to bind RNA(13). Although there is not a specific orthologue of NS5A in the SARS-CoV-2 genome, their activities may be exerted by multiple other proteins.

Consistently, daclatasvir inhibited the production of infectious SARS-CoV-2 titers with EC_{50} values ranging from 0.6 to 1.1 µM across different cell types, including pneumocytes. The pharmacological parameters presented against SARS-CoV-2 are within the area under the curve (AUC) for dacaltasvir's pharmacokinetic in humans (12, 33), thus supporting its potential for clinical trials against COVID-19, according to drug prioritizing algorithms (34). Moreover, daclatasvir impaired SARS-CoV-2 RNA synthesis in Calu-3 cells, suggesting an action in the RNA polymerization complex, similarly to its activity on HCV.

Influenza A virus and other highly pathogenic respiratory viruses provoke cytokine storm, an exaggerated immune response leading to an uncontrolled pro-inflammatory cytokine response(35, 36). Similarly, severe COVID-19 is associated with cytokine storm (27), marked by increased IL-6 levels (27). Dacaltasvir diminished cell-associated viral RNA in human primary monocytes and not only IL-6, but also TNF-α levels, another hallmark of this hyper-inflammation (27, 37), and it was more potent than atazanavir, previously showed by us to inhibit SARS-CoV-2 (38).

With respect to sofosbuvir, although the architecture of the SARS-CoV-2 and HCV RNA polymerase nucleotide uptake channel is similar (23), the 2'-Me radical apparently bumps onto critical amino acid residues on the enzymes structure (24). In enzyme kinetic assays with SARS-CoV-2 nsp7, 8 and 12, its RNA polymerase complex, sofosbuvir-triphosphate, the active metabolite, competitively acts as a chain terminator(24, 25). Similarly, RBV-, favipiravir- and RDV-triphosphate also target SARS-CoV-2 RNA elongation (24, 25). Indeed, sofosbuvir reduced the RNA synthesis in SARS-CoV-2-infected cells.

However, to become active in biological systems, sofosbuvir, the pro-drug, must be converted to its above mentioned triphosphate. This is a multi-stage pathway in which hydrophobic protections in the monophosphate of sofosbuvir are removed by liver enzymes CatA, CES1 and HINT1(19). Nevertheless, according to the Human Protein Atlas, these enzymatic entities are also found in the respiratory tract (20–22). Indeed, we found that SARS-CoV-2 replication could be inhibited by sofosbuvir, at high concentrations in HuH-7 hepatoma cells and Calu-3 type II pneumocytes. It is impossible to compare sofosbuvir efficacy over HCV and SARS-CoV-2 because assays readout are quite different,

respectively: replication systems and PFU. There is a limited knowledge on the intracellular concentration of sofosbuvir in anatomical compartments other than the liver. Based on the classical plasma pharmacokinetic model (19), the SFV's potencies for SARS-CoV-2 would not be physiological.

The time-frame for antiviral intervention could be up to the 10 days after onset of illness, which overlaps with the clinical deterioration of COVID-19, marked by the severe respiratory dysfunction (27). Therefore, there is a therapeutic window that can be explored, as long as an active antiviral agent is available. It is expected that early antiviral intervention will modulate the uncontrolled pro-inflammatory cytokine storm, allowing an equilibrated adaptive immune response towards resolution of the infection. Early antiviral intervention may lead to the breakdown of the deleterious cycle triggered by SARS-CoV-2 and improve patients' clinical outcomes. Thus, our data on anti-HCV drugs, in especial daclatasvir, could reinforce their indication as a potential compounds for clinical trials.

4) Material and Methods

4.1. Reagents.

The antiviral Lopinavir/ritonavir (4:1 proportion) was pruchased from AbbVie (Ludwingshafen, Germany). Chloroquine, atazanavir, ritonavir and ribavirin were received as donations from Instituto de Tecnologia de Fármacos (Farmanguinhos, Fiocruz). Atazanavir/ritonavir was used in the proportion 3:1. Daclatasvir and Sofosbuvir were donated by Microbiologica Química-Farmacêutica LTDA (Rio de Janeiro, Brazil). ELISA assays were purchased from R&D Bioscience. All small molecule inhibitors were dissolved in 100% dimethylsulfoxide (DMSO) and subsequently diluted at least 10^4-fold in culture or reaction medium before each assay. The final DMSO concentrations showed no cytotoxicity. The materials for cell culture were purchased from Thermo Scientific Life Sciences (Grand Island, NY), unless otherwise mentioned.

4.2. Cells and Virus

African green monkey kidney (Vero, subtype E6), human hepatoma (Huh-7), human lung epithelial cell lines (A549 and Calu-3) cells were cultured in high glucose DMEM with 10% fetal bovine serum (FBS; HyClone, Logan, Utah), 100 U/mL penicillin and 100 µg/mL streptomycin (Pen/Strep; ThermoFisher) at 37 °C in a humidified atmosphere with 5% CO_2.

Human primary monocytes were obtained after 3 h of plastic adherence of peripheral blood mononuclear cells (PBMCs). PBMCs were isolated from healthy donors by density gradient centrifugation (Ficoll-Paque, GE Healthcare). PBMCs (2.0×10^6 cells) were plated onto 48-well plates (NalgeNunc) in RPMI-1640 without serum for 2 to 4 h. Non-adherent cells were removed and the remaining monocytes were maintained in DMEM with 5% human serum (HS; Millipore) and penicillin/streptomycin. The purity of human monocytes was above 95%, as determined by flow cytometric analysis (FACScan; Becton Dickinson) using anti-CD3 (BD Biosciences) and anti-CD16 (Southern Biotech) monoclonal antibodies. The experimental procedures using involving human cells were performed with samples obtained after written informed consent and were approved by the Institutional

Review Board (IRB) of the Oswaldo Cruz Foundation/Fiocruz (Rio de Janeiro, RJ, Brazil) under the number 397-07, to the author DCBH.

SARS-CoV-2 was prepared in Vero E6 cells at MOI of 0.01. Originally, the isolate was obtained from a nasopharyngeal swab from a confirmed case in Rio de Janeiro, Brazil (IRB approval, 30650420.4.1001.0008). All procedures related to virus culture were handled in a biosafety level 3 (BSL3) multiuser facility according to WHO guidelines. Virus titers were determined as plaque forming units (PFU)/mL. Virus stocks were kept in - 80 °C ultralow freezers.

4.3. Cytotoxicity assay

Monolayers of 1.5 x 10^4 cells in 96-well plates were treated for 3 days with various concentrations (semi-log dilutions from 1000 to 10 µM) of the antiviral drugs. Then, 5 mg/ml 2,3-bis-(2-methoxy-4-nitro-5-sulfophenyl)-2*H*-tetrazolium-5-carboxanilide (XTT) in DMEM was added to the cells in the presence of 0.01% of N-methyl dibenzopyrazine methyl sulfate (PMS). After incubating for 4 h at 37 °C, the plates were measured in a spectrophotometer at 492 nm and 620 nm. The 50% cytotoxic concentration (CC_{50}) was calculated by a non-linear regression analysis of the dose–response curves.

4.4. Yield-reduction assay

Unless otherwise mentioned, Vero cells were infected with a multiplicity of infection (MOI) of 0.01. HuH-7, A549 and Calu-3 were infected at MOI of 0.1. Cells were infected at densities of 5 x 10^5 cells/well in 48-well plates for 1h at 37 °C. The cells were washed, and various concentrations of compounds were added to DMEM with 2% FBS. After 24 or 48h, supernatants were collected and harvested virus was quantified by PFU/mL or real time RT-PCR. A variable slope non-linear regression analysis of the dose-response curves was performed to calculate the concentration at which each drug inhibited the virus production by 50% (EC_{50}).

For time-of-addition assays, 5 x 10^5 vero cells/well in 48-well plates wee infected with MOI of 0.01 for 1h at 37 °C. Treatments started from 2h before to 18h after infection with two-times EC_{50} concentration. On the next day, culture supernatants were collected and tittered by PFU/mL.

4.5. Virus titration

Monolayers of Vero cells (2 x 10^4 cell/well) in 96-well plates were infected with serial dilutions of supernatants containing SARS-CoV-2 for 1h at 37°C. Cells were washed, fresh medium added with 2% FBS and 3 to 5 days post infection the cytopathic effect was scored in at least 3 replicates per dilution by independent readers. The reader was blind with respect to source of the supernatant.

4.6. Molecular detection of virus RNA levels.

The total RNA from a culture was extracted using QIAamp Viral RNA (Qiagen®), according to manufacturer's instructions. Quantitative RT-PCR was performed using QuantiTect Probe RT-PCR Kit (Quiagen®) in an ABI PRISM 7500 Sequence Detection System (Applied Biosystems). Amplifications were carried out in 25 µL reaction mixtures containing 2× reaction mix buffer, 50 µM of each primer, 10 µM of probe, and 5 µL of RNA template. Primers, probes, and cycling conditions recommended by the Centers for Disease Control and Prevention (CDC) protocol were used to detect the SARS-CoV-2(39). The standard curve method was employed for virus quantification. For reference to the cell amounts used, the housekeeping gene RNAse P was amplified. The Ct values for this target were compared to those obtained to different cell amounts, 10^7 to 10^2, for calibration. Alternatively, genomic (ORF1) and subgenomic (ORFE) were detected, as described elsewhere (40).

4.7. Statistical analysis

The assays were performed blinded by one professional, codified and then read by another professional. All experiments were carried out at least three independent times, including a minimum of two technical replicates in each assay. The dose-response curves used to calculate EC_{50} and CC_{50} values were generated by variable slope plot from Prism GraphPad software 8.0. The equations to fit the best curve were generated based on R^2 values $\geq$ 0.9. Student's T-test was used to access statistically significant *P* values <0.05. The statistical analyses specific to each software program used in the bioinformatics analysis are described above.

Acknowledgments

Thanks are due to Prof. Andrew Hill from the University of Liverpool and Dr. James Freeman from the GP2U Telehealth for simulative scientific debate. Dr. Carmen Beatriz Wagner Giacoia Gripp from Oswaldo Cruz Institute is acknowledged for assessments related to BSL3 facility. Dr. Andre Sampaio from Farmanguinhos, platform RPT11M, is acknowledged for kindly donate the Calu-3 cells. We thank the Hemotherapy Service of the Hospital Clementino Fraga Filho (Federal University of Rio de Janeiro, Brazil) for providing buffy-coats. This work was supported by Conselho Nacional de Desenvolvimento Científico e Tecnológico (CNPq), Fundação de Amparo à Pesquisa do Estado do Rio de Janeiro (FAPERJ). This study was financed in part by the Coordenac□ão de Aperfeic□oamento de Pessoal de Nível Superior - Brasil (CAPES) - Finance Code 001. Funding was also provided by CNPq, CAPES and FAPERJ through the National Institutes of Science and Technology Program (INCT) to Carlos Morel (INCT-IDPN). Thanks are due to Oswaldo Cruz Foundation/FIOCRUZ under the auspicious of Inova program. The funding sponsors had no role in the design of the study; in the collection, analyses, or interpretation of data; in the writing of the manuscript, and in the decision to publish the results.

References

1. Masters PS. 2006. The molecular biology of coronaviruses. Adv Virus Res 66:193–292.

2. Cui J, Li F, Shi Z-L. 2019. Origin and evolution of pathogenic coronaviruses. Nat Rev Microbiol 17:181–192.

3. Dong E, Du H, Gardner L. 2020. An interactive web-based dashboard to track COVID-19 in real time. Lancet Infect Dis 0.

4. Harrison C. 2020. Coronavirus puts drug repurposing on the fast track. Nat Biotechnol.

399 5. Organization WH. 2020. WHO R&D Blueprint: informal consultation on prioritization of
400 candidate therapeutic agents for use in novel coronavirus 2019 infection, Geneva,
401 Switzerland, 24 January 2020. WHO/HEO/R & D Blueprint (nCoV)/2020.1.

402 6. Borba MGS, Val FFA, Sampaio VS, Alexandre MAA, Melo GC, Brito M, Mourão MPG, Brito-
403 Sousa JD, Baía-da-Silva D, Guerra MVF, Hajjar LA, Pinto RC, Balieiro AAS, Pacheco AGF, Santos
404 JDO, Naveca FG, Xavier MS, Siqueira AM, Schwarzbold A, Croda J, Nogueira ML, Romero GAS,
405 Bassat Q, Fontes CJ, Albuquerque BC, Daniel-Ribeiro C-T, Monteiro WM, Lacerda MVG. 2020.
406 Effect of High vs Low Doses of Chloroquine Diphosphate as Adjunctive Therapy for Patients
407 Hospitalized With Severe Acute Respiratory Syndrome Coronavirus 2 (SARS-CoV-2) Infection:
408 A Randomized Clinical Trial. JAMA Netw Open 3:e208857–e208857.

409 7. Wang Y, Zhang D, Du G, Du R, Zhao J, Jin Y, Fu S, Gao L, Cheng Z, Lu Q, Hu Y, Luo G, Wang K,
410 Lu Y, Li H, Wang S, Ruan S, Yang C, Mei C, Wang Y, Ding D, Wu F, Tang X, Ye X, Ye Y, Liu B,
411 Yang J, Yin W, Wang A, Fan G, Zhou F, Liu Z, Gu X, Xu J, Shang L, Zhang Y, Cao L, Guo T, Wan Y,
412 Qin H, Jiang Y, Jaki T, Hayden FG, Horby PW, Cao B, Wang C. 2020. Remdesivir in adults with
413 severe COVID-19: a randomised, double-blind, placebo-controlled, multicentre trial. The
414 Lancet 395:1569–1578.

415 8. Cao B, Wang Y, Wen D, Liu W, Wang J, Fan G, Ruan L, Song B, Cai Y, Wei M, Li X, Xia J, Chen N,
416 Xiang J, Yu T, Bai T, Xie X, Zhang L, Li C, Yuan Y, Chen H, Li H, Huang H, Tu S, Gong F, Liu Y, Wei
417 Y, Dong C, Zhou F, Gu X, Xu J, Liu Z, Zhang Y, Li H, Shang L, Wang K, Li K, Zhou X, Dong X, Qu Z,
418 Lu S, Hu X, Ruan S, Luo S, Wu J, Peng L, Cheng F, Pan L, Zou J, Jia C, Wang J, Liu X, Wang S, Wu
419 X, Ge Q, He J, Zhan H, Qiu F, Guo L, Huang C, Jaki T, Hayden FG, Horby PW, Zhang D, Wang C.
420 2020. A Trial of Lopinavir-Ritonavir in Adults Hospitalized with Severe Covid-19. N Engl J Med.

9. Goldman JD, Lye DCB, Hui DS, Marks KM, Bruno R, Montejano R, Spinner CD, Galli M, Ahn M-Y, Nahass RG, Chen Y-S, SenGupta D, Hyland RH, Osinusi AO, Cao H, Blair C, Wei X, Gaggar A, Brainard DM, Towner WJ, Muñoz J, Mullane KM, Marty FM, Tashima KT, Diaz G, Subramanian A. 2020. Remdesivir for 5 or 10 Days in Patients with Severe Covid-19. N Engl J Med 0:null.

10. Beigel JH, Tomashek KM, Dodd LE, Mehta AK, Zingman BS, Kalil AC, Hohmann E, Chu HY, Luetkemeyer A, Kline S, Lopez de Castilla D, Finberg RW, Dierberg K, Tapson V, Hsieh L, Patterson TF, Paredes R, Sweeney DA, Short WR, Touloumi G, Lye DC, Ohmagari N, Oh M, Ruiz-Palacios GM, Benfield T, Fätkenheuer G, Kortepeter MG, Atmar RL, Creech CB, Lundgren J, Babiker AG, Pett S, Neaton JD, Burgess TH, Bonnett T, Green M, Makowski M, Osinusi A, Nayak S, Lane HC. 2020. Remdesivir for the Treatment of Covid-19 — Preliminary Report. N Engl J Med 0:null.

11. De Clercq E, Li G. 2016. Approved Antiviral Drugs over the Past 50 Years. Clin Microbiol Rev 29:695–747.

12. Smith MA, Regal RE, Mohammad RA. 2016. Daclatasvir: A NS5A Replication Complex Inhibitor for Hepatitis C Infection. Ann Pharmacother 50:39–46.

13. Gordon DE, Jang GM, Bouhaddou M, Xu J, Obernier K, O'Meara MJ, Guo JZ, Swaney DL, Tummino TA, Hüttenhain R, Kaake RM, Richards AL, Tutuncuoglu B, Foussard H, Batra J, Haas K, Modak M, Kim M, Haas P, Polacco BJ, Braberg H, Fabius JM, Eckhardt M, Soucheray M, Bennett MJ, Cakir M, McGregor MJ, Li Q, Naing ZZC, Zhou Y, Peng S, Kirby IT, Melnyk JE, Chorba JS, Lou K, Dai SA, Shen W, Shi Y, Zhang Z, Barrio-Hernandez I, Memon D, Hernandez-Armenta C, Mathy CJP, Perica T, Pilla KB, Ganesan SJ, Saltzberg DJ, Ramachandran R, Liu X,

Rosenthal SB, Calviello L, Venkataramanan S, Lin Y, Wankowicz SA, Bohn M, Trenker R, Young JM, Cavero D, Hiatt J, Roth T, Rathore U, Subramanian A, Noack J, Hubert M, Roesch F, Vallet T, Meyer B, White KM, Miorin L, Agard D, Emerman M, Ruggero D, García-Sastre A, Jura N, Zastrow M von, Taunton J, Schwartz O, Vignuzzi M, d'Enfert C, Mukherjee S, Jacobson M, Malik HS, Fujimori DG, Ideker T, Craik CS, Floor S, Fraser JS, Gross J, Sali A, Kortemme T, Beltrao P, Shokat K, Shoichet BK, Krogan NJ. 2020. A SARS-CoV-2-Human Protein-Protein Interaction Map Reveals Drug Targets and Potential Drug-Repurposing. bioRxiv 2020.03.22.002386.

14. Keating GM. 2014. Sofosbuvir: a review of its use in patients with chronic hepatitis C. Drugs 74:1127–1146.

15. de Freitas CS, Higa LM, Sacramento CQ, Ferreira AC, Reis PA, Delvecchio R, Monteiro FL, Barbosa-Lima G, James Westgarth H, Vieira YR, Mattos M, Rocha N, Hoelz LVB, Leme RPP, Bastos MM, L Rodrigues GO, M Lopes CE, Queiroz-Junior CM, Lima CX, Costa VV, Teixeira MM, Bozza FA, Bozza PT, Boechat N, Tanuri A, Souza TML. 2019. Yellow fever virus is susceptible to sofosbuvir both in vitro and in vivo. PLoS Negl Trop Dis 13:e0007072.

16. Ferreira AC, Reis PA, de Freitas CS, Sacramento CQ, Villas Boas Hoelz L, Bastos MM, Mattos M, Rocha N, Gomes de Azevedo Quintanilha I, da Silva Gouveia Pedrosa C, Rocha Quintino Souza L, Correia Loiola E, Trindade P, Rangel Vieira Y, Barbosa-Lima G, de Castro Faria Neto HC, Boechat N, Rehen SK, Bruning K, Bozza FA, Bozza PT, Souza TML. 2018. Beyond members of the Flaviviridae family, sofosbuvir also inhibits chikungunya virus replication. Antimicrob Agents Chemother.

17. Ferreira AC, Zaverucha-do-Valle C, Reis PA, Barbosa-Lima G, Vieira YR, Mattos M, Silva P de P, Sacramento C, Neto HCCF, Campanati L, Tanuri A, Brüning K, Bozza FA, Bozza PT, Souza TML. 2017. Sofosbuvir protects Zika virus-infected mice from mortality, preventing short- and long-term sequelae. Sci Rep 7:9409.

18. Sacramento CQ, de Melo GR, de Freitas CS, Rocha N, Hoelz LV, Miranda M, Fintelman-Rodrigues N, Marttorelli A, Ferreira AC, Barbosa-Lima G, Abrantes JL, Vieira YR, Bastos MM, de Mello Volotão E, Nunes EP, Tschoeke DA, Leomil L, Loiola EC, Trindade P, Rehen SK, Bozza FA, Bozza PT, Boechat N, Thompson FL, de Filippis AM, Brüning K, Souza TM. 2017. The clinically approved antiviral drug sofosbuvir inhibits Zika virus replication. Sci Rep 7:40920.

19. SOVALDI (sofosbuvir) monograph. Available on http://www.gilead.ca/application/files/8015/6330/6529/Sovaldi_English_PM_e162880-GS-008.pdf, acessed on 15-Jul-2020

20. Tissue expression of CTSA - Staining in lung - The Human Protein Atlas. Available on https://www.proteinatlas.org/ENSG00000064601-CTSA/tissue, acessed on 15-Jul-2020

21. Tissue expression of CES1 - Summary - The Human Protein Atlas. Available on https://www.proteinatlas.org/ENSG00000198848-CES1/tissue, acessed on 15-Jul-2020

22. Tissue expression of HINT1 - Summary - The Human Protein Atlas. Available on https://www.proteinatlas.org/ENSG00000169567-HINT1/tissue, acessed on 15-Jul-2020

23. Gao Y, Yan L, Huang Y, Liu F, Zhao Y, Cao L, Wang T, Sun Q, Ming Z, Zhang L, Ge J, Zheng L, Zhang Y, Wang H, Zhu Y, Zhu C, Hu T, Hua T, Zhang B, Yang X, Li J, Yang H, Liu Z, Xu W, Guddat LW, Wang Q, Lou Z, Rao Z. 2020. Structure of the RNA-dependent RNA polymerase from COVID-19 virus. Science 368:779–782.

24. Gordon CJ, Tchesnokov EP, Woolner E, Perry JK, Feng JY, Porter DP, Gotte M. 2020. Remdesivir is a direct-acting antiviral that inhibits RNA-dependent RNA polymerase from severe acute respiratory syndrome coronavirus 2 with high potency. J Biol Chem jbc.RA120.013679.

25. Ju J, Kumar S, Li X, Jockusch S, Russo JJ. 2020. Nucleotide Analogues as Inhibitors of Viral Polymerases. bioRxiv 2020.01.30.927574.

26. Mesci P, Macia A, Saleh A, Martin-Sancho L, Yin X, Snethlage C, Avansini S, Chanda SK, Muotri A. 2020. Sofosbuvir protects human brain organoids against SARS-CoV-2. bioRxiv 2020.05.30.125856.

27. Zhou F, Yu T, Du R, Fan G, Liu Y, Liu Z, Xiang J, Wang Y, Song B, Gu X, Guan L, Wei Y, Li H, Wu X, Xu J, Tu S, Zhang Y, Chen H, Cao B. 2020. Clinical course and risk factors for mortality of adult inpatients with COVID-19 in Wuhan, China: a retrospective cohort study. The Lancet 395:1054–1062.

28. Newton AH, Cardani A, Braciale TJ. 2016. The host immune response in respiratory virus infection: balancing virus clearance and immunopathology. Semin Immunopathol 38:471–482.

29. Dong E, Du H, Gardner L. 2020. An interactive web-based dashboard to track COVID-19 in real time. Lancet Infect Dis 0.

30. Lin L, Lu L, Cao W, Li T. 2020. Hypothesis for potential pathogenesis of SARS-CoV-2 infection-a review of immune changes in patients with viral pneumonia. Emerg Microbes Infect 9:727–732.

507 31. Li H, Liu L, Zhang D, Xu J, Dai H, Tang N, Su X, Cao B. 2020. SARS-CoV-2 and viral sepsis:
508 observations and hypotheses. The Lancet 395:1517–1520.

509 32. Figueiredo-Mello C, Casadio LVB, Avelino-Silva VI, Yeh-Li H, Sztajnbok J, Joelsons D, Antonio
510 MB, Pinho JRR, Malta F de M, Gomes-Gouvêa MS, Salles APM, Corá AP, Moreira CHV, Ribeiro
511 AF, Nastri AC de SS, Malaque CMS, Teixeira RFA, Borges LMS, Gonzalez MP, Junior LCP, Souza
512 TNL, Song ATW, D'Albuquerque LAC, Abdala E, Andraus W, Martino RB de, Ducatti L,
513 Andrade GM, Malbouisson LMS, Souza IM de, Carrilho FJ, Sabino EC, Levin AS. 2019. Efficacy
514 of sofosbuvir as treatment for yellow fever: protocol for a randomised controlled trial in
515 Brazil (SOFFA study). BMJ Open 9:e027207.

516 33. Gandhi Y, Eley T, Fura A, Li W, Bertz RJ, Garimella T. 2018. Daclatasvir: A Review of Preclinical
517 and Clinical Pharmacokinetics. Clin Pharmacokinet 57:911–928.

518 34. Arshad U, Pertinez H, Box H, Tatham L, Rajoli RK, Curley P, Neary M, Sharp J, Liptrott NJ,
519 Valentijn A, David C, Rannard SP, O'Neill PM, Aljayyoussi G, Pennington S, Ward SA, Hill A,
520 Back DJ, Khoo SH, Bray PG, Biagini GA, Owen A. 2020. Prioritisation of Anti-SARS-Cov-2 Drug
521 Repurposing Opportunities Based on Plasma and Target Site Concentrations Derived from
522 their Established Human Pharmacokinetics. Clin Pharmacol Ther.

523 35. Gao R, Bhatnagar J, Blau DM, Greer P, Rollin DC, Denison AM, Deleon-Carnes M, Shieh WJ,
524 Sambhara S, Tumpey TM, Patel M, Liu L, Paddock C, Drew C, Shu Y, Katz JM, Zaki SR. 2013.
525 Cytokine and chemokine profiles in lung tissues from fatal cases of 2009 pandemic influenza
526 A (H1N1): role of the host immune response in pathogenesis. Am J Pathol 183:1258–68.

527 36. Peschke T, Bender A, Nain M, Gemsa D. 1993. Role of macrophage cytokines in influenza A
528 virus infections. Immunobiology 189:340–55.

529 37. Monteerarat Y, Sakabe S, Ngamurulert S, Srichatraphimuk S, Jiamtom W, Chaichuen K,
530 Thitithanyanont A, Permpikul P, Songserm T, Puthavathana P, Nidom CA, Mai le Q, Iwatsuki-
531 Horimoto K, Kawaoka Y, Auewarakul P. 2010. Induction of TNF-alpha in human macrophages
532 by avian and human influenza viruses. Arch Virol 155:1273–9.

533 38. Fintelman-Rodrigues N, Sacramento CQ, Lima CR, Silva FS da, Ferreira A, Mattos M, Freitas
534 CS de, Soares VC, Dias S da SG, Temerozo JR, Miranda M, Matos AR, Bozza FA, Carels N, Alves
535 CR, Siqueira MM, Bozza PT, Souza TML. 2020. Atazanavir inhibits SARS-CoV-2 replication and
536 pro-inflammatory cytokine production. bioRxiv 2020.04.04.020925.

537 39. CDC. 2020. Coronavirus Disease 2019 (COVID-19). Cent Dis Control Prev.

538 40. Wölfel R, Corman VM, Guggemos W, Seilmaier M, Zange S, Müller MA, Niemeyer D, Jones
539 TC, Vollmar P, Rothe C, Hoelscher M, Bleicker T, Brünink S, Schneider J, Ehmann R,
540 Zwirglmaier K, Drosten C, Wendtner C. 2020. Virological assessment of hospitalized patients
541 with COVID-2019. 7809. Nature 581:465–469.

542

Author contributions

Experimental execution and analysis – CQS, NFR, JRT, SSGD, ACF, MM, CRRP, CSF, VCS

Data analysis, manuscript preparation and revision – CQS, NFR, JRT, FAB, DCBH, PTB, TMLS

Conceptualized the experiments – NFR, CQS, JRT, TMLS

Study coordination – TMLS

Manuscript preparation and revision – DCBH, PTB, TMLS

The authors declare no competing financial interests.

Legend for the Figures

Figure 1. **The antiviral activity of daclatasvir and sofosbuvir (SFV) against SARS-CoV-2.** Vero (A and B), HuH-7 (C) or Calu-3 (D) cells, at density of 5 x 10^5 cells/well in 48-well plates, were infected with SARS-CoV-2, for 1h at 37 °C. Inoculum was removed, cells were washed and incubated with fresh DMEM containing 2% fetal bovine serum (FBS) and the indicated concentrations of the daclatasvir, SFV, chloroquine (CQ), lopinavir/ritonavir (LPV+RTV) or ribavirin (RBV). Vero (A and B) were infected with MOI of 0.01 and supernatants were accessed after 24 h. HuH-7 and Calu-3 cells were infected with MOI of 0.1 and supernatants were accessed after 48 h. Viral replication in the culture supernatant was measured by PFU/mL (A, C and D) or RT-PCR (B). The data represent means ± SEM of three independent experiments.

Figure 2. Daclatasvir and sofosbuvir (SFV) reduced SARS-CoV-2 associated RNA synthesis. (A) To initially understand the temporal pattern of inhibition promoted daclatasvir, we performed by Time-of-addition assays. Vero cells were infected with MOI 0f 0.01 of SARS-CoV-2 and treated with daclatasvir or ribavirin (RBV) with two-times their EC_{50} values at different times after infection, as indicated. After 24h post infection, culture supernatant was harvested and SARS-CoV-2 replication measured by plaque assay. (B) Next, Calu-3 cells (5 x 10^5 cells/well in 48-well plates), were infected with SARS-CoV-2 at MOI of 0.1, for 1h at 37 °C. Inoculum was removed, cells were washed and incubated with fresh DMEM containing 2% fetal bovine serum (FBS) and the indicated concentrations of the daclatasvir, SFV or ribavirin (RBV) at 10 µM. After 48h, cells monolayers were lysed, total RNA extracted and quantitative RT-PCR performed for detection of ORF1 and ORFE mRNA. The data represent means ± SEM of three independent experiments. * $P< 0.05$ for comparisons with vehicle (DMSO). # $P< 0.05$ for differences in genomic and sub-genomic RNA.

Figure 3. Daclatasvir impairs SARS-CoV-2 replication and cytokine storm in human primary monocytes. Human primary monocytes were infected at the MOI of 0.01 and treated with 1 µM of daclatasvir, chloroquine (CQ), atazanavir (ATV) or atazanavir/ritonavir (ATV+RTV). After 24h, cell-associated virus RNA loads (A), as well as TNF-α (B) and IL-6 (C) levels in the culture supernatant were measured. The data

represent means ± SEM of experiments with cells from at least three healthy donors. Differences with $P < 0.05$ are indicates (*), when compared to untreated cells (nil).

Table 1 – The pharmacological parameters of SARS-CoV-2 infected cell in the presence of daclatasvir and sofosbuvir (SFV)

	Daclatasvir				Sofosbuvir				Ribavirin				Chloroquine				LPV+RTV			
	EC50	EC90	CC50	SI	EC50	EC90	CC50	SI	EC50	EC90	CC50	SI	EC50	EC90	CC50	SI	EC50	EC90	CC50	SI
Vero/PFU	0.8 ± 0.3	3.4 ± 1.2	31 ± 8	39	>10	>10	360 ± 43	ND	ND	ND	ND	NA	1.3 ± 0.4	6.8 ± 0.3	268 ± 23	206	3.3 ± 0.2	7.3 ± 0.3	291 ± 32	88
Vero/Copies	>10	>10	31 ± 8	NA	>10	>10	421 ± 34	ND	ND	ND	ND	NA	0.9 ± 0.3	5.7 ± 0.2	268 ± 23	206	2.8 ± 0.5	9.8 ± 1.2	291 ± 32	104
Huh-7/PFU	0.6 ± 0.2	6.1 ± 1.4	28 ± 5	47	6.2 ± 1.1	10.8 ± 2.3	381 ± 34	61	6.5 ± 1.3	10 ± 0.3	142	13	ND	ND	ND	NA	2.9 ± 0.2	6.4 ± 0.3	328 ± 16	113
Calu-3/PFU	1.1 ± 0.3	3.0 ± 1.8	38 ± 5	34	9.5 ± 1.5	>10	512 ± 34	54	8.6 ± 1.3	>10	160	16	ND	ND	ND	NA	4.2 ± 0.5	9.8 ± 1.2	256 ± 17	61

EC50, EC90 and CC50 are described in µM

LPV+RTV stands for lopinavir/ritonavir

Figure 1

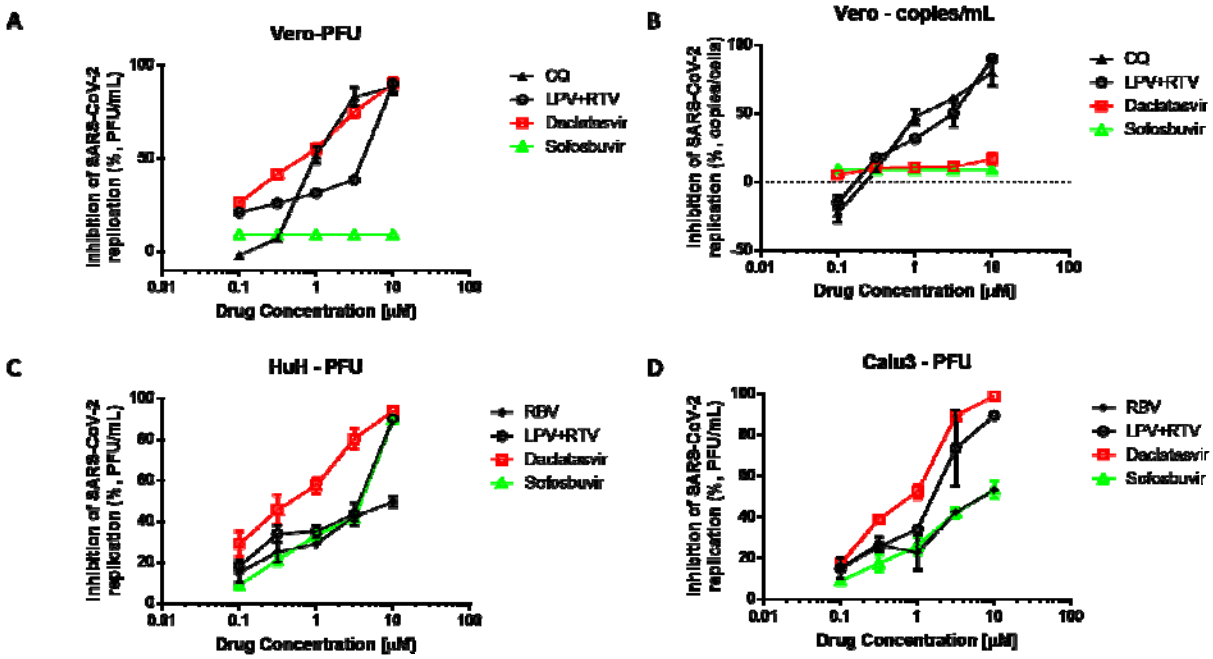

649

650

651 Figure 2A

652

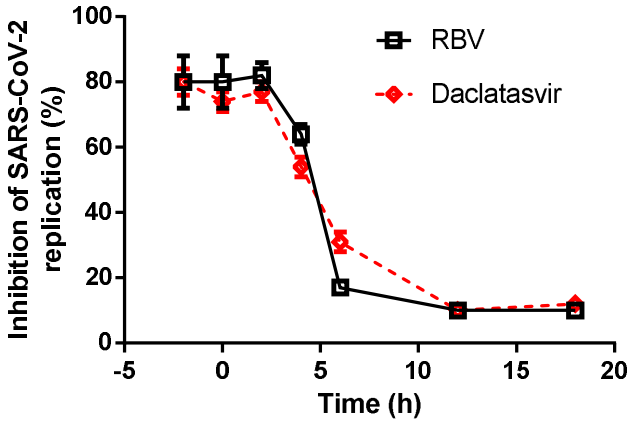

653

654

655 Figure 2B

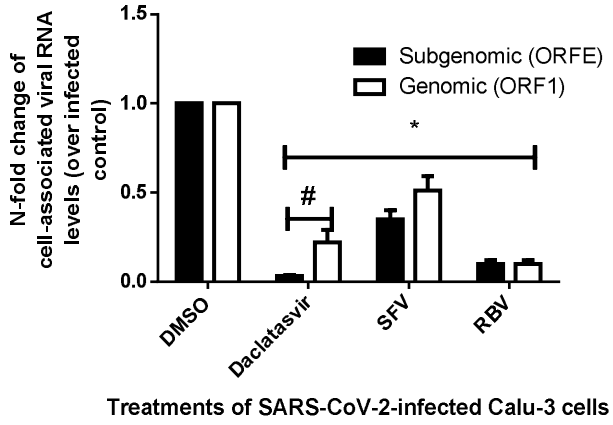

656

657

658

659

660

661

662

663

664

Figure 3